

# Flexural behavior of concrete slabs with corroded bars

Lou Chung<sup>a</sup>, Husam Najm<sup>b,\*</sup>, Perumalsamy Balaguru<sup>b</sup>

<sup>a</sup> *Department of Civil Engineering, Dankook University, Seoul, South Korea*

<sup>b</sup> *Department of Civil and Environmental Engineering, Rutgers, The State University of New Jersey, 98 Brett Road, Piscataway, NJ 08854, USA*

Received 3 January 2007; received in revised form 4 August 2007; accepted 8 August 2007

Available online 17 August 2007

## Abstract

Experimental and analytical evaluations of concrete slabs reinforced with corroded and uncorroded bars are presented. Seventy simply supported slabs reinforced with 10 mm diameter bars were tested in bending using a four-point load setup. The primary variables were the bond length and the corrosion level. The bond lengths varied from 10 to 440 mm and corrosion levels ranged from 0% to 4.6% diameter loss. The moment capacity of the slabs was also predicted using results from pull-out tests conducted on corroded bars in a separate study. The results indicate that the behavior of the slabs with corroded reinforcement can be predicted with good accuracy. As in the case of pull-out tests, a small amount of corrosion increases the flexural capacity of the slab. But the capacity reduces considerably when the loss in bar diameter exceeds 2%. The results confirm the hypothesis that bond deterioration is the major contributor to the reduction of moment capacity.

© 2007 Elsevier Ltd. All rights reserved.

**Keywords:** Corrosion; Diameter loss; Bond strength; Bending strength; Moment capacity

## 1. Introduction

Deterioration of reinforced concrete due to corrosion of reinforcement is a worldwide problem that affects a large number of reinforced concrete structures. Reduced strength and poor durability of corroded reinforced concrete members are a concern to many transportation agencies and building officials in the US and around the world. The estimate for the repair and rehabilitation of infrastructures in the US exceeds several billion dollars [11]. Industrialized countries in Europe, Asia and developing countries are also facing similar problems. Extensive research is being conducted on this subject on various fronts. These efforts can be broadly classified as (1) understanding the corrosion mechanism, (2) monitoring the behavior of reinforced concrete structures in the laboratory and in the field, (3) predicting the behavior of structural elements with corroded reinforcement, (4) finding ways to increase the ser-

vice life of structures, and (5) repair and rehabilitation and deterioration of structures [1,3,4]. Corrosion in the field usually results in localized corrosion in the form of pitting and simulating field conditions of corrosion in the laboratory is an approximate process. The loss of flexural strength due to this localized form of corrosion is insignificant. However, over time, pitting corrosion is likely to extend to other areas of the bar resulting in relatively uniform corrosion along the surface of the reinforcement [13]. Field corrosion is a more complex phenomenon and simulating field corrosion conditions in the laboratory would require complex and long-term testing procedures. The method used to induce corrosion in this study is a simple method that induces uniform corrosion along the longitudinal bars.

The results presented in this paper focus on the prediction of the behavior of flexural members with corroded reinforcement. In spite of the large number of publications available in the area of corrosion, information on the behavior of structural elements with corroded reinforcement is limited [5–7,13]. The limited number of available studies concludes that corrosion results in strength

\* Corresponding author.

E-mail address: [hnajm@rci.rutgers.edu](mailto:hnajm@rci.rutgers.edu) (H. Najm).

reduction due to loss of cross-sectional area and loss of bond between concrete and reinforcement. The influence of bond deterioration is much more critical than the loss of cross-sectional area [13]. For example, a loss of 5% of area of reinforcement will result in only 5% tension force reduction but more than 80% loss of bond strength could occur. Therefore, a research program was initiated by the Korean Science Foundation as a joint effort by Dankook University in Korea and Rutgers University in the United States to study the influence of corrosion on bond deterioration and subsequent strength loss in beams (slabs) and columns. The bond properties of corroded bars, evaluated in a separate study [8,9] using pull-out prismatic specimens in tension showed that corrosion results in considerable bond strength reduction. If there is more than 2% reduction in diameter, corrosion reduces both strength and slip at failure considerably. If the corrosion is less than 1%, corrosion improves the bond properties [5,8,9]. Estimating the load carrying capacity of a corroded reinforced concrete member and predicting the remaining life of the structure is needed by many agencies and to address safety and performance issues and to design repair and rehabilitation programs for their structures. This study evaluates the effect of corrosion on bond deterioration and subsequent loss of strength in slab specimens and the correlation between the results of the pull-out tests [9] and slab specimens. Seventy slab specimens, specially designed to evaluate the effect of corrosion on bond, were tested in flexure using four-point loading. The analysis of results shows that there is very good correlation between the results of the pull-out tests and slab specimens tests.

## 2. Experimental program

### 2.1. Specimens details

The test specimens consisted of 500 mm wide, 1200 mm long, and 90 mm thick slabs reinforced with three sets of bars. The first set of bars, designated as E, was placed near the edges and covered the entire length of the slab excluding the 50 mm clear covers at both ends. The bar placed at the middle, designated as A, was terminated at a short distance to the left of the maximum moment point (loading point) as shown in Fig. 1. The distance between the maximum loading point and the end of the bar, considered as the development length, was one of the primary variables of this investigation. The third set of bars, designated as B, was placed on either side of bar A, and was terminated on the right side of the loading points. Here again, the difference between the maximum load point and the end of the bars was varied to induce bond failure.

Note that the setup does not have any hooks that would interfere with bond length evaluation and no lateral reinforcement that could interfere with the accelerated corrosion process. Hooks and transverse reinforcement were not part of this study. This study is a first step in evaluating the effect of corrosion on flexural strength and the effect of

corrosion on flexural strength in the presence of hooks and stirrups need to be evaluated in future studies. The geometry of the slab and reinforcement details was chosen to induce bond failure in some of the bars.

Larger bar diameters were not used because they would result in spalling cracks in the concrete cover due to expansion caused by higher corrosion levels. The 10 mm diameter also provides more uniform bond distribution along the bar and the maximum load can be maintained at large slip values. These characteristics are critical for estimating the bond strength of corroded bars embedded in the slab. This aspect is explained further in the analysis section.

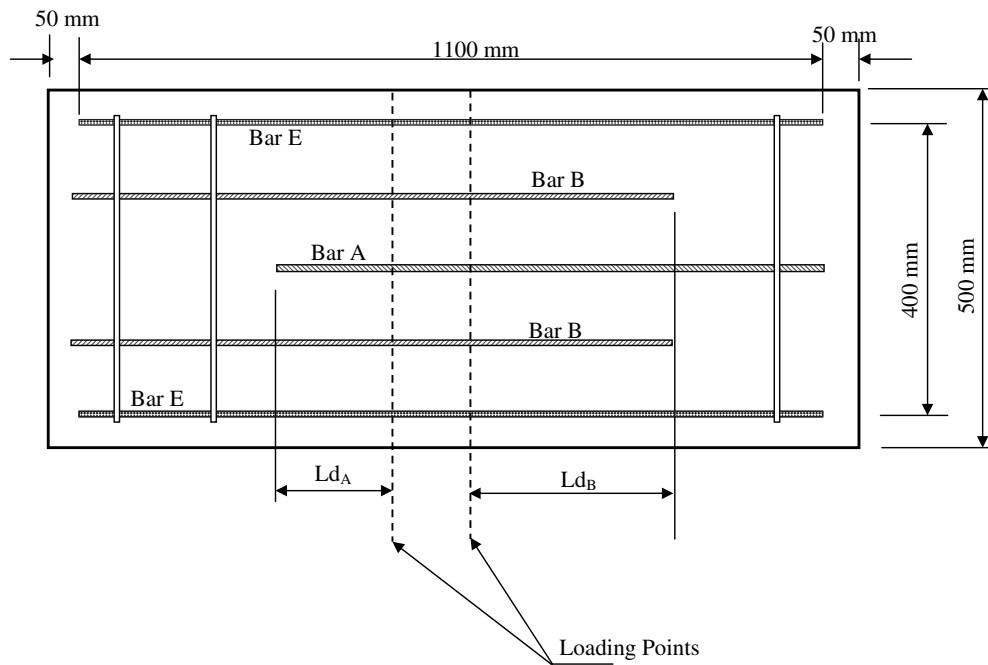
### 2.2. Test parameters

The development lengths of bars A and B varied from 10 mm to 440 mm. A development length of about 150 mm was needed for the uncorroded bars to develop their yield strength. Development lengths that are much shorter and larger than 150 mm were chosen for this study to obtain comprehensive data. The specimens were divided into three series: Series I, Series II, and Series III. In Series I, the development length varied from 10 mm to 110 mm and the corrosion levels were low and were kept under 1% diameter loss. The corrosion level was expressed as a percentage reduction in bar diameter for comparison with other published results. In this series, most specimens failed by pullout of bars A and B. In Series II, the development length varied from 30 mm to 330 mm (300% the development length of Series I). In this series, a fraction of specimens failed by debonding and some failed by yielding of steel. The corrosion level of this series was medium and was equal to 1.16% diameter loss. In Series III, the development length was increased to 440 mm and the corrosion levels were high and they varied from 1.7% to 4.6% diameter loss. Specimen details, corrosion levels, and the development lengths of Series I, II, and III are presented in Tables 1–3 respectively.

### 2.3. Mixing, casting and curing of specimens

The constituent materials for concrete were Portland cement, sand, and 9 mm maximum size coarse aggregate. The target compressive strength was 21 MPa. The low strength was chosen to obtain a concrete that is more conducive for accelerated corrosion. The water–cement ratio was 0.55. Cement, fine and coarse aggregate contents were 309, 800 and 976 kg/m<sup>3</sup> respectively. A chloride-based accelerating admixture was added at the dosage of 1.55 kg/m<sup>3</sup>. The slump was 150 mm. The reinforcement consisted of 10 mm diameter deformed bars, which had similar surface characteristics of ASTM 615 # 3 bars.

A laboratory concrete mixer was used for mixing using the following sequence. First, coarse and fine aggregates were loaded and soaked with two-thirds of the water for 1 min to allow for absorption of water. Then cement, remaining water, and the admixture were added and mixed



S - 1 - 4 - 15

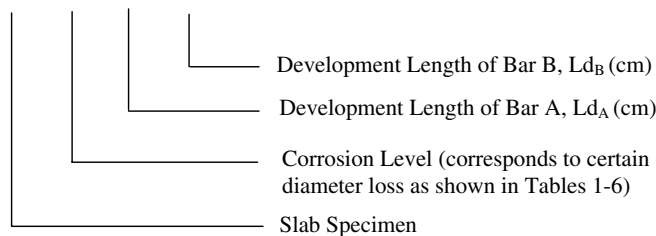


Fig. 1. Details of slab specimens.

for 3 min. After a rest period of 3 min, mixing was continued for an additional 2 min. The slab specimens were cast using specially prepared molds. The reinforcement was placed at the proper location using plastic spacers. Special care was taken to ensure the effective cover of 35 mm. Release agent was used to aid easy removal of slabs from the forms, and compaction was achieved using vibration. At the end of casting, polyethylene sheets were used to cover the samples for 24 h. Companion  $100 \times 200$  mm cylinders were also cast for compressive strength measurements. In order to obtain uniform and accelerated corrosion, the corrosion process was started at 14 days. The slabs were soaked in a 3% NaCl solution before placing them in corrosion chamber. Conditioning and corrosion procedures were similar to the procedures used for pull-out tests conducted earlier in a separate study [8,9].

#### 2.4. Test setup

The slabs were tested using a four point bending test as shown in Fig. 2. The slabs were simply supported over a span of 1000 mm with two loads applied at 450 mm from

the supports. Strain in the top the concrete was measured by strain gages placed at top of slab at midspan in the middle of the slab over bar A. The loads were applied using displacement control testing machine. The load was measured using a load cell and the mid-span deflection was measured using an LVDT. Crack patterns were also monitored.

#### 3. Current induced corrosion

Constant current accelerated corrosion was induced externally by applying a direct electric current [2,9]. The current is passed from the reinforcement to the copper plate to induce corrosion. The schematic diagram is shown in Fig. 3. Direct current supply was used with the positive output connected to the reinforcement and the negative output connected to the copper plate. The current flow was recorded using a computer. The amount of corrosion (loss of mass), which is a function of the direct current amperage and time interval, can be expressed using the following equation:

Table 1  
Details of specimens with low corrosion level

| Specimen designation | Corrosion level (%) | Development length A (mm) | Development length B (mm) |
|----------------------|---------------------|---------------------------|---------------------------|
| S 0-1-5              | 0                   | 10                        | 50                        |
| S 0-2-7              | 0                   | 20                        | 70                        |
| S 0-3-9              | 0                   | 30                        | 90                        |
| S 0-5-11             | 0                   | 50                        | 110                       |
| S 0-7-1              | 0                   | 70                        | 10                        |
| S 0-9-2              | 0                   | 90                        | 20                        |
| S 0-11-3             | 0                   | 110                       | 30                        |
| S 1-1-5              | 0.58                | 10                        | 50                        |
| S 1-1-2              | 0.58                | 20                        | 70                        |
| S 1-3-9              | 0.58                | 30                        | 90                        |
| S 1-5-11             | 0.58                | 50                        | 110                       |
| S 1-7-1              | 0.58                | 70                        | 10                        |
| S 1-9-2              | 0.58                | 90                        | 20                        |
| S 1-11-3             | 0.58                | 110                       | 30                        |
| S 2-1-5              | 0.87                | 10                        | 50                        |
| S 2-2-7              | 0.87                | 20                        | 70                        |
| S 2-3-9              | 0.87                | 30                        | 90                        |
| S 2-5-11             | 0.87                | 50                        | 110                       |
| S 2-7-1              | 0.87                | 70                        | 10                        |
| S 2-11-2             | 0.87                | 90                        | 20                        |
| S 2-11-3             | 0.87                | 110                       | 30                        |

Corrosion level values given are percentage diameter loss.

Table 2  
Details of specimens of Series II with moderate corrosion level

| Specimen designation | Corrosion level (%) | Development length A (mm) | Development length B (mm) |
|----------------------|---------------------|---------------------------|---------------------------|
| S 0-3-15             | 0                   | 30                        | 150                       |
| S 0-6-21             | 0                   | 60                        | 210                       |
| S 0-9-27             | 0                   | 90                        | 270                       |
| S 0-15-33            | 0                   | 150                       | 330                       |
| S 0-21-3             | 0                   | 210                       | 30                        |
| S 0-27-6             | 0                   | 270                       | 60                        |
| S 3-3-15             | 1.16                | 30                        | 150                       |
| S 3-6-21             | 1.16                | 60                        | 210                       |
| S 3-9-27             | 1.16                | 90                        | 270                       |
| S 3-15-33            | 1.16                | 150                       | 330                       |
| S 3-21-3             | 1.16                | 210                       | 30                        |
| S 3-27-6             | 1.16                | 270                       | 60                        |

Corrosion level values given are percentage diameter loss.

$$\text{Mass Loss (g)} = \frac{it56(\text{g})}{(2)(96,500)} \quad (1)$$

Eq. (1) is based on Faraday's Law where the constant 56 represents the molar mass of iron (atomic weight). For each mole of oxidized ions, 2 moles of electrons are given out, consuming a charge of  $2 \times 96,500$  coulombs (Amp-sec) and  $i$  is the current in amp and  $t$  is the time in seconds. There is an excellent correlation between actual mass loss and theoretical mass loss predicted using Eq. (1) [9,12]. The corrosion level was expressed as percent loss of bar diameter defined as the corrosion penetration (mm) divided by the original diameter (mm) multiplied by 100.

Using Eq. (1), the percent loss of bar diameter can be expressed as

Table 3  
Details of specimens of Series III with high corrosion levels

| Specimen designation | Corrosion level (%) | Development length A (mm) | Development length B (mm) |
|----------------------|---------------------|---------------------------|---------------------------|
| S 0-4-20             | 0                   | 40                        | 200                       |
| S 0-8-28             | 0                   | 80                        | 280                       |
| S 0-12-36            | 0                   | 120                       | 360                       |
| S 0-20-44            | 0                   | 200                       | 440                       |
| S 0-28-4             | 0                   | 280                       | 40                        |
| S 0-36-8             | 0                   | 360                       | 80                        |
| S 0-44-12            | 0                   | 440                       | 120                       |
| S 5-4-20             | 1.7                 | 40                        | 200                       |
| S 5-8-28             | 1.7                 | 80                        | 280                       |
| S 5-12-36            | 1.7                 | 120                       | 360                       |
| S 5-20-44            | 1.7                 | 200                       | 440                       |
| S 5-28-4             | 1.7                 | 280                       | 40                        |
| S 5-36-8             | 1.7                 | 360                       | 80                        |
| S 5-44-12            | 1.7                 | 440                       | 120                       |
| S 7-4-20             | 2.3                 | 40                        | 200                       |
| S 7-8-28             | 2.3                 | 80                        | 280                       |
| S 7-12-36            | 2.3                 | 120                       | 360                       |
| S 7-20-44            | 2.3                 | 200                       | 440                       |
| S 7-28-4             | 2.3                 | 280                       | 40                        |
| S 7-36-8             | 2.3                 | 360                       | 80                        |
| S 7-44-12            | 2.3                 | 440                       | 120                       |
| S 10-4-20            | 3.2                 | 40                        | 200                       |
| S 10-8-28            | 3.2                 | 80                        | 280                       |
| S 10-12-36           | 3.2                 | 120                       | 360                       |
| S 10-20-44           | 3.2                 | 200                       | 440                       |
| S 10-28-4            | 3.2                 | 280                       | 40                        |
| S 10-36-8            | 3.2                 | 360                       | 80                        |
| S 10-44-12           | 3.2                 | 440                       | 120                       |
| S 15-4-20            | 4.6                 | 40                        | 200                       |
| S 15-8-28            | 4.6                 | 80                        | 280                       |
| S 15-12-36           | 4.6                 | 120                       | 360                       |
| S 15-20-44           | 4.6                 | 200                       | 440                       |
| S 15-28-4            | 4.6                 | 280                       | 40                        |
| S 15-36-8            | 4.6                 | 360                       | 80                        |
| S 15-44-12           | 4.6                 | 440                       | 120                       |

Corrosion level values given are percentage diameter loss.

$$\text{Bar diameter loss (\%)} = \frac{3197it}{(0.5 d)} \times 100 \quad (2)$$

where  $i$  is the corrosion current density (A/mm<sup>2</sup>),  $t$  is corrosion time interval (days), and  $d$  is the bar diameter (mm).

#### 4. Test results and discussion

As mentioned earlier, the test program was designed to isolate the influence of corrosion on bond properties and the resulting strength reduction. The load-deflection responses of the 70 test specimens were analyzed to estimate the bond deterioration caused by various levels of corrosion. The critical parameters were flexural stiffness of uncracked slabs, cracking moment (load), maximum moment, and reduction in toughness. There is a considerable difference between typical reinforced concrete slabs and the slabs tested in this investigation, for the purpose estimating maximum moment. Since in most cases, three out of five reinforcing bars could fail by debonding, rather



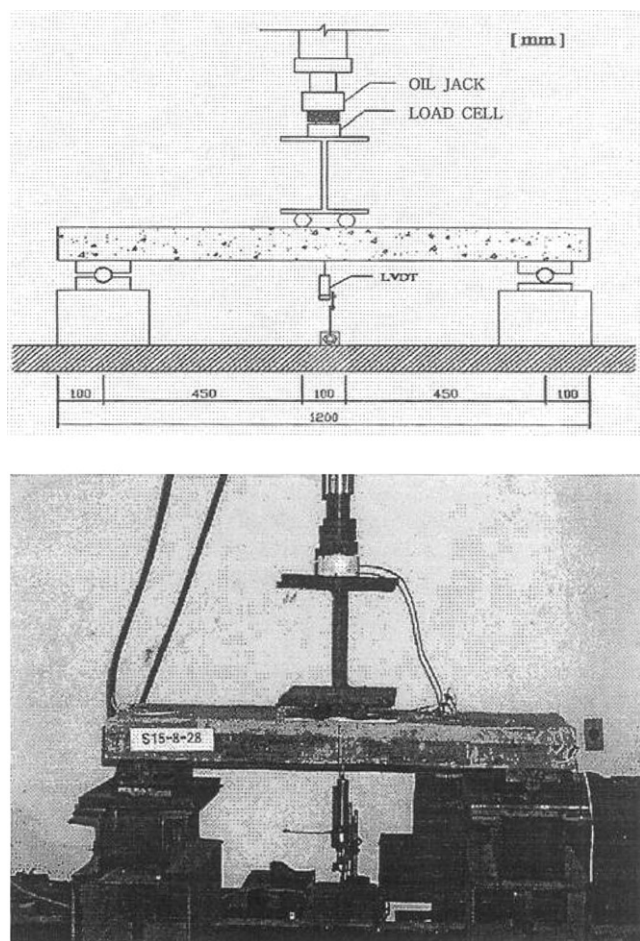


Fig. 2. Induced corrosion setup.

than yielding, the moment at first yield provides the maximum moment. This aspect is further explained in a later section.

## 5. Flexural stiffness of uncracked slab and cracking moment

A careful review of all the 70 load-deflection responses indicates that corrosion did not affect either the stiffness or the cracking moment. This should be expected because the expansion caused by corrosion products of 10 mm diameter bars is not sufficient to crack the slab. Even at high corrosion levels, the bars still maintain some bond strength provided by frictional resistance of the concrete surface rather than by mechanical interlocking.

The average compressive strength of companion cylinders was 19 MPa. Using an estimated value of 2.7 MPa for the modulus of rupture [10] and gross moment of inertia of  $30.4 \times 10^6 \text{ mm}^4$ , the cracking moment,  $M_{cr}$ , of the concrete alone was equal to 1.82 kN m. For the load set-up used in this investigation, this cracking moment translates to a cracking load of 8.1 kN. This value is consistent with the experimental results. Note that the effect of reinforcement was neglected, and hence the reinforcement details do not influence the cracking moment.

## 6. Overall load–deflection behavior and maximum loads

Typical load–deflection behavior of slabs with uncorroded and corroded reinforcement is shown in Figs. 4 and 5 respectively. The load–deflection behavior depended on the reinforcement details. As expected, Fig. 4 shows that maximum measured loads decreased with reduced development length. When the three bars in the middle part of the slab (bars A and B) did not have sufficient bond length, the maximum (failure) load was smaller and it occurred at a much lower deflection. This also indicated that the edge bars (bars E), which had sufficient bond length, did not undergo extensive yielding at maximum loads. Fig. 4 also shows the effect of development length on bending stiffness and toughness. As the bond length increased, the maximum load increased and the flexural stiffness in post-cracking and pre-yield regions also increased. The figure shows that the slab behaved like a typical under reinforced slab when bars A and B were long (specimen S0-20-44).

The effect of corrosion on the flexural behavior of reinforced concrete slabs is shown in Fig. 5. From the load deflection curves in Fig. 5, it can be seen that corrosion decreases the maximum load, the post-cracking flexural stiffness, and the load capacity at large deflections. This figure also shows the effect of corrosion on toughness. As the level of corrosion increases, the flexural toughness decreases. For high corrosion levels, the decrease in flexural toughness is significant. The results in Table 6 show that for medium and high corrosion levels, the magnitude of the maximum load was not significantly different despite the increase in bond lengths of bars A and B. This indicates that the primary reason for the loss of strength and stiffness in reinforced concrete slabs tested in this study is primarily due to loss of bond at the interface due to corrosion and not due to loss in bar area.

### 6.1. Maximum loads

The maximum loads obtained experimentally are presented in Tables 4–6 for Series I (low corrosion), Series II (medium corrosion), and Series III (high corrosion) respectively. These tables also show the maximum load ratio which is the ratio of the predicted maximum load to the measured maximum load. As mentioned earlier, specimens subjected to low level corrosion had bars with smaller bond lengths. Bond lengths were increased for specimens subjected to high level corrosion. Note that even at high levels of corrosion, the loss of area and the corresponding tension force reduction is not significant (less than 10%). The reduction of reinforcing bar diameter due to corrosion was also shown by other researchers [13] to be insignificant compared to loss of bond. A careful review of the results of the slab specimens tested in this study leads to the following observations: (1) as in the case of pull-out specimens [8,9], low level corrosion increases the load capacity.

Note that, at zero corrosion, one or three bars (bars A and B) had a lower pullout load compared to slabs

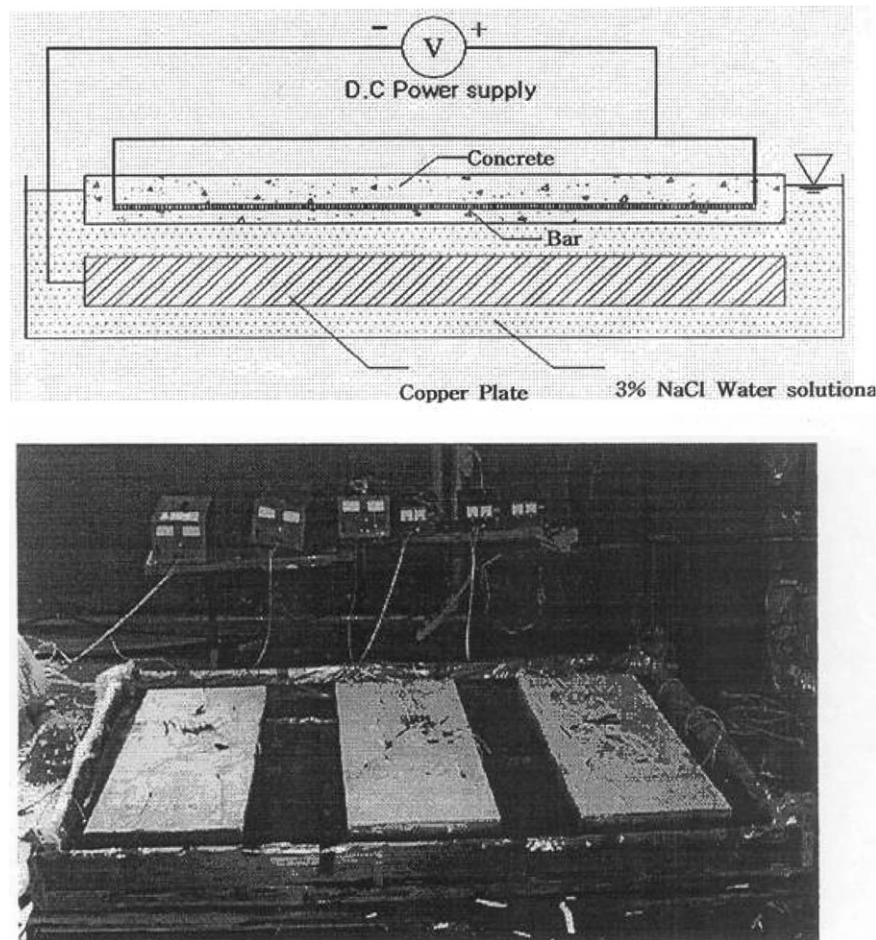


Fig. 3. Test setup.

with slightly corroded bars. The change in the contribution of fully embedded bars is negligible. The increase occurred in 10 out of 14 specimens, (2) when the corrosion level increased to 1.16% diameter loss, there was load capacity reduction in three specimens and slight increase in two specimens. The increase was much smaller when compared to specimens corroded at 0.58% and 0.87% diameter losses.

This trend was the same as the one observed in pull-out tests on corroded and uncorroded specimens [8,9]. The increase in bond strength due to corrosion levels-off at about 1% diameter loss, (3) once the corrosion level was increased to 1.7% diameter loss and higher, all the specimens showed a decrease in maximum load capacity. The decrease is substantial at 4.6% diameter loss. For these specimens, the bond lengths were increased to account for loss of bond force due to corrosion. In spite of this increase, there was more than 40% decrease in some cases. Similar reductions in flexural strength of reinforced concrete beams were observed by other researchers [13] for the same corrosion levels, and (4) the decrease in load capacity for corroded specimens between 3.2% and 4.6% diameter loss was substantial for all specimens tested with such high corrosion levels.

## 7. Analytical investigation

The experimental investigation was carefully designed so that the load carrying capacities of the slabs can be estimated using the results of pull-out tests conducted by Auyeung et al. [8,9] and the basic principles of mechanics. When the slabs reached their load carrying capacity, some bars were pulling out and the bars with sufficient bond length yielded. The analytical procedure presented below is based on the following assumptions:

1. The maximum load occurs at the onset of yielding of bars with sufficient bond length. Since 10 mm diameter bars can sustain maximum bond loads at large slips [8,9], the contribution of bars with insufficient bond lengths were calculated using the bond strength and the embedment length. The bond strengths for various corrosion levels were taken from the average bond strength versus percent corrosion levels curve obtained from pull-out tests conducted by Auyeung et al. [8,9].
2. The strain distribution across the thickness of the slab was assumed to be linear.
3. The behavior of concrete was assumed to be linearly elastic. This assumption was verified using the maximum

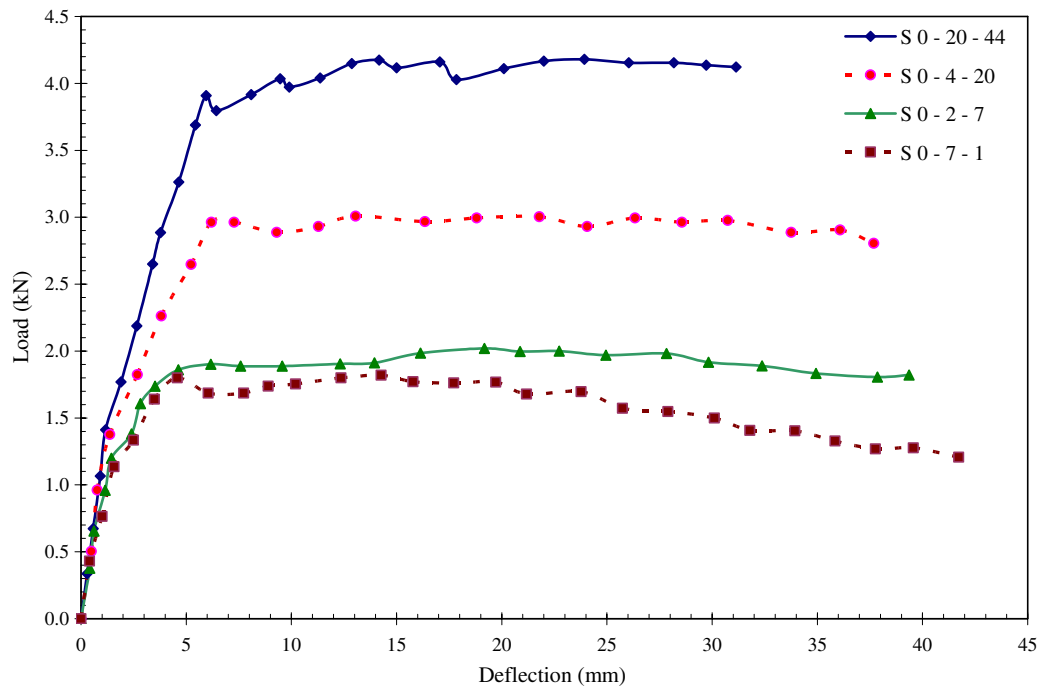


Fig. 4. Load–deflection behavior: specimens with no corrosion.

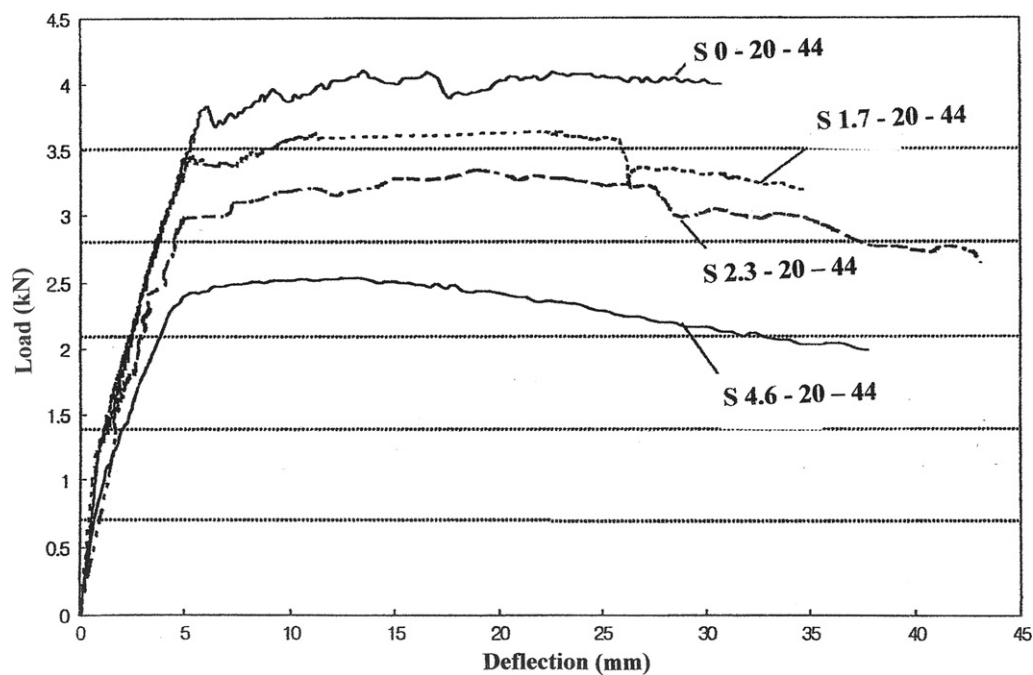


Fig. 5. Load–deflection behavior: specimens with corrosion.

concrete strains at peak load. The maximum strains were less than 0.001, and hence this assumption is valid.

### 7.1. Procedure

Based on the assumption presented in the previous section, a cracked section analysis was conducted to obtain

the maximum load. The depth of neutral axis was computed using the force equilibrium equation. If the depth of neutral axis is  $kd$ , the compressive force,  $C$  can be calculated as

$$C = \frac{1}{2} b k d f'_{\text{cmax}} \quad (3)$$



Table 4  
Maximum loads of specimens of Series I with low corrosion levels

| Specimen designation | Corrosion level (% diameter loss) | Measured Pmax (kN) | Predicted Pmax (kN) | Maximum load ratio |
|----------------------|-----------------------------------|--------------------|---------------------|--------------------|
| S 0-1-5              | 0                                 | 2.45               | 2.14                | 0.87               |
| S 1-1-5              | 0.58                              | 2.47               | 2.22                | 0.90               |
| S 2-1-5              | 0.87                              | 2.63               | 2.24                | 0.85               |
| S 0-2-7              | 0                                 | 2.05               | 2.39                | 1.17               |
| S 1-2-7              | 0.58                              | 2.19               | 2.50                | 1.14               |
| S 2-2-7              | 0.87                              | 2.73               | 2.55                | 0.93               |
| S 0-3-9              | 0                                 | 2.15               | 2.64                | 1.23               |
| S 1-3-9              | 0.58                              | 2.94               | 2.76                | 0.94               |
| S 2-3-9              | 0.87                              | 2.83               | 2.85                | 1.01               |
| S 0-5-11             | 0                                 | 2.51               | 2.94                | 1.17               |
| S 1-5-11             | 0.58                              | 2.58               | 3.12                | 1.20               |
| S 2-5-11             | 0.87                              | 2.63               | 3.20                | 1.21               |
| S 0-7-1              | 0                                 | 1.87               | 2.04                | 1.09               |
| S 1-7-1              | 0.58                              | 1.72               | 2.12                | 1.23               |
| S 2-7-1              | 0.87                              | 2.7                | 2.15                | 0.80               |
| S 0-9-2              | 0                                 | 3.15               | 2.25                | 0.71               |
| S 1-9-2              | 0.58                              | 1.84               | 2.44                | 1.32               |
| S 2-9-2              | 0.87                              | 3.08               | 2.48                | 0.81               |
| S 0-11-3             | 0                                 | 2.61               | 2.44                | 0.94               |
| S 1-11-3             | 0.58                              | 1.82               | 2.54                | 1.39               |
| S 2-11-3             | 0.87                              | 2.63               | 1.60                | 0.99               |

Table 5  
Maximum loads of specimens of Series II with moderate corrosion level

| Specimen designation | Corrosion level (% diameter loss) | Measured Pmax (kN) | Predicted Pmax (kN) | Maximum load ratio |
|----------------------|-----------------------------------|--------------------|---------------------|--------------------|
| S 0-3-15             | 0                                 | 2.98               | 3.22                | 1.08               |
| S 3-3-15             | 1.16                              | 3.00               | 3.18                | 1.06               |
| S 0-6-21             | 0                                 | 3.57               | 3.37                | 0.94               |
| S 3-6-21             | 1.16                              | 3.43               | 3.35                | 0.98               |
| S 0-9-27             | 0                                 | 3.59               | 3.52                | 0.98               |
| S 3-9-27             | 1.16                              | 3.89               | 3.52                | 0.91               |
| S 0-21-3             | 0                                 | 2.90               | 2.64                | 0.91               |
| S 3-21-3             | 1.16                              | 2.61               | 2.60                | 1.00               |
| S 0-27-6             | 0                                 | 3.12               | 2.94                | 0.94               |
| S 3-27-6             | 1.16                              | 2.67               | 2.95                | 1.10               |

where  $b$  is the width of the slab and  $f'_{\text{cmax}}$  is the maximum compressive stress. Since the concrete is assumed to be linearly elastic,  $f'_{\text{cmax}}$  in Eq. (3) can be replaced by  $E_c \varepsilon_{\text{max}}$  where  $E_c$  is the elastic modulus of concrete and  $\varepsilon_{\text{max}}$  is the maximum concrete strain.

$$C = \frac{1}{2} b k d E \varepsilon_{\text{max}} \quad (4)$$

Since the load is calculated on the onset of yielding, the strain  $\varepsilon_{\text{max}}$  can be expressed as a function yield strain of steel,  $\varepsilon_y$  and depth of neutral axis.

$$\frac{\varepsilon_{\text{max}}}{\varepsilon_y} = \frac{kd}{d - kd} \quad (5)$$

$$C = \frac{1}{2} b E_c \varepsilon_y \frac{(kd)^2}{d - kd} \quad (6)$$

The tension force consists of the summation of yield capacity of certain bars and maximum pullout load of short bars. Therefore, the tension force,  $T$  is calculated as

Table 6  
Maximum loads of specimens of Series III with high corrosion levels

| Specimen designation | Corrosion level (% diameter loss) | Measured Pmax (kN) | Predicted Pmax (kN) | Maximum load ratio |
|----------------------|-----------------------------------|--------------------|---------------------|--------------------|
| S 0-4-20             | 0                                 | 3.40               | 3.31                | 0.97               |
| S 5-4-20             | 1.7                               | 2.67               | 3.17                | 1.18               |
| S 10-4-20            | 3.2                               | 2.99               | 2.44                | 0.82               |
| S 15-4-20            | 4.6                               | 1.92               | 1.67                | 0.87               |
| S 0-8-28             | 0                                 | 3.89               | 3.46                | 0.89               |
| S 5-8-28             | 1.7                               | 3.35               | 3.35                | 1.00               |
| S 7-8-28             | 2.3                               | 3.66               | 3.29                | 0.90               |
| S 10-8-28            | 3.2                               | 3.35               | 2.85                | 0.85               |
| S 15-8-28            | 4.6                               | 2.65               | 1.92                | 0.72               |
| S 0-12-36            | 0                                 | 4.10               | 3.63                | 0.89               |
| S 5-12-36            | 1.7                               | 3.53               | 3.55                | 1.01               |
| S 10-12-36           | 3.2                               | 3.27               | 3.15                | 0.96               |
| S 15-12-36           | 4.6                               | 2.39               | 2.21                | 0.93               |
| S 0-20-44            | 0                                 | 4.09               | 3.80                | 0.93               |
| S 5-20-44            | 1.7                               | 3.63               | 3.68                | 1.01               |
| S 7-20-44            | 3.2                               | 3.35               | 3.65                | 1.09               |
| S 15-20-44           | 4.6                               | 2.54               | 2.46                | 0.97               |
| S 0-28-4             | 0                                 | 2.94               | 2.74                | 0.93               |
| S 5-28-4             | 1.7                               | 2.59               | 2.64                | 1.02               |
| S 7-28-4             | 2.3                               | 2.72               | 2.41                | 0.89               |
| S 10-28-4            | 3.2                               | 2.43               | 2.31                | 1.95               |
| S 15-28-4            | 4.6                               | 1.72               | 1.59                | 0.92               |
| S 0-36-8             | 0                                 | 2.82               | 3.12                | 1.11               |
| S 5-36-8             | 1.7                               | 2.58               | 3.02                | 1.17               |
| S 7-36-8             | 2.3                               | 2.08               | 2.74                | 1.31               |
| S 10-36-8            | 3.2                               | 2.63               | 2.37                | 0.90               |
| S 15-36-8            | 4.6                               | 1.83               | 1.77                | 0.97               |
| S 0-44-12            | 0                                 | 3.64               | 3.52                | 0.97               |
| S 5-44-12            | 1.7                               | 3.30               | 3.40                | 1.03               |
| S 7-44-12            | 2.3                               | 3.06               | 3.07                | 1.00               |
| S 10-44-12           | 3.2                               | 2.56               | 2.48                | 0.97               |
| S 15-44-12           | 4.6                               | 1.95               | 2.00                | 1.03               |

$$T = \sum \frac{\pi}{4} d_b^2 f_y + \sum \pi d_b l_b f_b \quad (7)$$

where  $d_b$  is the diameter of the bar,  $f_y$  is the yield strength of steel,  $l_b$  is the embedment length of the bar, and  $f_b$  is the bond strength. Note that  $(\pi d_b l_b f_b)$  cannot exceed  $(0.25 \pi d_b^2 f_y)$ . Since  $C$  is equal to  $T$ , then:

$$b E_c \varepsilon_y (kd)^2 = (d - kd) \left( \sum \frac{\pi}{2} d_b^2 f_y + \sum 2 \pi d_b l_b f_b \right) \quad (8)$$

The quadratic equation in (8) was solved to obtain the depth of neutral axis and the nominal moment capacity,  $M_n$ , was obtained using Eq. (9):

$$M_n = T \left( d - \frac{kd}{3} \right) \quad (9)$$

Eq. (9) was used to estimate the maximum load for the four point loading setup shown in Fig. 3. The compressive strength was 19 MPa for all slabs based on the cylinder tests. This strength and ACI code equation was used for estimating the elastic modulus as 20.4 GPa. The yield strength of bars was taken as 414 MPa. The bond strength  $f_b$  was obtained from pull-out tests on corroded and uncorroded bars conducted in a separate study [8,9]. These values were: 6.6, 7.1, 6.7, 5.5, 5.0, 2.5 and 1.3 MPa for corrosion levels 0%, 0.58%, 0.87%, 1.16%, 1.7%, 2.3%,



3.2% and 4.6% diameter loss respectively. The geometric details, bond lengths, and various corrosion levels were used for estimating the maximum loads. For the corroded bars, the reduced area of cross section was used for the computation of yield strength.

## 8. Results and discussion

The measured maximum loads from the experimental results and the predicted maximum loads from the analytical results are shown in Tables 4–6 for low corrosion, medium corrosion, and high corrosion respectively. A graphical representation of these loads is shown in Fig. 6. Tables 4–6 and Fig. 6 show that the predicted maximum loads are in agreement with the measured loads. The fact that the tests on bond specimens and slab specimens were conducted in two different countries and average compressive strengths were used for all the slabs adds to the validity of analytical procedure. The error for specimens with corrosion level equal to 1.16% loss of diameter varied from 2% to 10% as shown in the last column in Table 5. The average error for these specimens was about 6%. The average error for specimens with uncorroded bars was about 1.5%. For the remaining specimens, the errors were: 16%, 6%, 1%, 6%, 4%, 9% and 8% for corrosion levels 0.58%, 0.87%, 1.16%, 1.7%, 2.3%, 3.2%, and 4.6% diameter loss respectively. Among the various corrosion levels, there was no consistency in under or over prediction. The average error for all the corroded specimens is less than 1%. The coefficient of variation for uncorroded and corroded specimens were 12.5% and 14.3%, respectively.

The results show that there is an excellent correlation between bond strength loss and moment capacity loss.

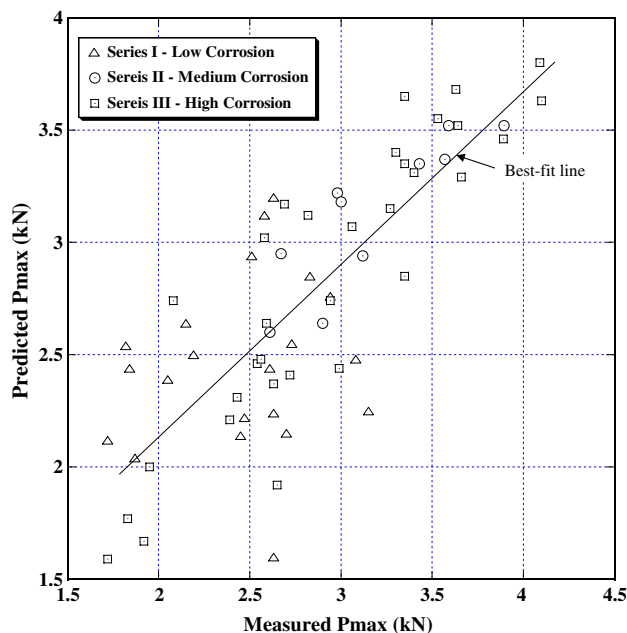


Fig. 6. Comparison of measured and predicted maximum loads.

Consistent accuracy for bond lengths varying from 20 mm to 50 mm and corrosion levels up to 4.6% indicates that if the effect of corrosion on bond can be isolated, the capacity of flexural members with corroded reinforcement can be predicted with good accuracy. In actual structures, presence of lateral reinforcement and hooks makes it difficult to estimate this capacity. However, the results reported in this paper provide a good starting point. The results also confirm the widely accepted hypothesis that the loss of bond is more critical than the loss of the cross sectional area of tension reinforcement.

## 9. Conclusions

Seventy simply supported slab specimens reinforced with 10 mm diameter bars were tested in bending using a four-point load setup. The 10 mm bar size was selected to avoid spalling associated with larger bar diameters and to provide a more uniform bond distribution along the bar and to maintain the maximum load at large slip values. The results indicate that the behavior of the slabs with corroded reinforcement can be predicted with good accuracy and that a small amount of corrosion increases the flexural capacity of the slab, however, the capacity is reduced considerably when the loss in bar diameter exceeds 2%. The results confirm the hypothesis that bond deterioration is the major contributor to the reduction of moment capacity. From the experimental and analytical results obtained in this study, the following conclusions can be drawn:

1. As in the case of pull-out tests on corroded bars, a small amount of corrosion increases the load carrying capacity of slabs. This increase levels off when the corrosion level reaches about 1% diameter loss.
2. When the diameter loss exceeds 2%, the load carrying capacity of slab starts to decrease. Once the decreasing trend starts, the load carrying capacity drops at a rapid rate.
3. There is a good correlation between the pull-out tests and the slab tests. The behavior of slab could be predicted using the results of pull-out specimens. The authors believe the results presented in this paper is a starting point for developing analytical procedures that accounts for tension force reduction due to loss of bond resulting from corrosion.
4. The results confirm the hypothesis that the loss of tension force capacity due to bond deterioration is more critical than the force loss due to the decrease in cross sectional area of bars.

## References

- [1] Physical Assessment for Concrete Bridge Components Relative to Reinforcement Corrosion. SHRP Workshop December 1997.
- [2] Berke NS, Shen DF, Sundberg KM. Comparison of the polarization resistance technique to the Macrocell corrosion technique. In: Berke NS, Chaker V, Whiting D, editors. Corrosion rates of steel in

- concrete. ASTM STP, vol. 1065. Philadelphia: American Society for Testing and Materials. p. 38–51.
- [3] El-Jazairi B, Berke NS. The use of calcium nitrite as a corrosion inhibiting admixture to steel reinforcement in concrete. In: Page CL, Treadaway KWJ, Bamforth PB, editors. *Corrosion of reinforcement in concrete*. London: Elsevier Applied Science; 1990. p. 571–85.
- [4] Berke NS, Hicks MC, Hoopes RJ. Condition assessment of field structures with calcium nitrite. In: Weyers Richard E, editor. Philip D. Cady international symposium concrete bridges in aggressive environments. ACI SP, vol. 151. Detroit, MI: American Concrete Institute; 1994. p. 43–72.
- [5] Fu, Xuli, Chung DDL. Effect of water–cement ratio, curing age, silicafume, polymer admixture, steel surface treatments, and corrosion on bond, between concrete and steel reinforcing bars. *ACI Materials Journal* 1998;95-M72 (November–December):725–34.
- [6] Chapman Ralph A, Shah Surendra P. Early-Age Bond Strength in Reinforced concrete. *ACI Mater J* 1987;84(6):501–10.
- [7] Ezeldin AS, Balaguru P. Bond behavior of normal and high strength fiber reinforced concrete. *ACI Mater J* 1989;86(M49):515–24.
- [8] Auyeung Y, Balaguru P, Chung L. Bond behavior of corroded reinforcement. *Am Concrete Inst Mater J* 2000;97(2):214–20.
- [9] Auyeung Y, Balaguru P, Chung L. Influence of corrosion on the bond behavior of reinforcement bars. *ACI SP* 2000;193:1051–74.
- [10] ACI Committee 318. *Building code reinforcements for reinforced concrete (ACI 318-99)*. Detroit: American Concrete Institute, 1999, p. 111.
- [11] ASCE Report Card for America's Infrastructure. Progress Report September 2003, p. 1–7.
- [12] El-Maaddawy T, Soudki K. Effectiveness of impressed current technique to simulate corrosion of steel reinforcement in concrete. *ASCE, J Mater Civil Eng* 2003;15(1):41–7.
- [13] Mangat P, Elgarf M. Flexural strength of concrete beams with corroding reinforcement. *ACI Struct J* 1999;96(1):149–58.